Journal of Photochemistry and Photobiology A: Chemistry 208 (2009) 79–90

Contents lists available at ScienceDirect

Journal of Photochemistry and Photobiology A: Chemistry

journal homepage: www.elsevier.com/locate/jphotochem

Photo-oxidations initiated by UV radiation of urocanic acid and its methyl ester in solution, micelles, and lipid bilayers: TYPE I (free radical) or TYPE II (singlet oxygen) mechanisms depend on the medium

Amelia A. Rand, L. Ross C. Barclay*

Department of Chemistry, Mount Allison University, Sackville, New Brunswick, Canada E4L 1G8

ARTICLE INFO

Article history:
Received 14 July 2009
Received in revised form 19 August 2009
Accepted 27 August 2009
Available online 2 September 2009

Keywords:
Free radical peroxidation
Singlet oxygen
Micelles
Lipid bilayers
Mechanism

ABSTRACT

Photo-oxidative reactions on methyl linoleate (ML) initiated by UV radiation of urocanic acid (UCA) or methyl urocanate (UCAME) in a non-polar solvent, aqueous sodium dodecyl sulfate (SDS) micelles or ML in lipid bilayers of dimyristoylphosphatidylcholine (DMPC) or of dilinoleoylphosphatidylcholine (DLPC) are investigated to determine medium effects on reaction mechanisms. Experiments include: kinetics of oxygen uptake, effects of radical trapping antioxidants or singlet oxygen quenchers and product analysis of *cis,trans* to *trans,trans* (*c,t*//*t,t*) isomer ratios of oxidized linoleate to distinguish free radical, TYPE I and singlet oxygen TYPE II reactions. Irradiation of the system toluene/ML/UCAME reaction occurred by TYPE I according to kinetics studies and inhibiting effects of 2,6-di-*t*-butyl-4-methoxyphenol (DBHA) and the four typical *c,t*//*t,t* isomer ratios formed. Similarly irradiation of the system SDS/ML/UCAME (or UCA) resulted in the TYPE I reaction. The latter system was used to evaluate the antioxidant activities, k_{inh}, showing the relative activities as: Trolox ≥ 2,2,5,7,8-pentamethylhydroxychroman (PMHC) > DBHA. The low k_{inh} values of these antioxidants compared to those in a non-polar solvent are interpreted by quantitative methods of "solvent effects". Photo-oxidation of the systems DMPC/ML/UCA or DLPC/UCA occurred by singlet oxygen (TYPE II) in contrast to those in solution or micelles according to effects of a singlet oxygen quencher, sodium azide, and lack of inhibition by antioxidants. This contrast is explained by the structure of lipid bilayers where the excited ^{3}n,π* of UCA produces singlet oxygen in the aqueous phase which diffuses into the bilayer phase to cause TYPE II reactions.

1. Introduction

Urocanic acid (UCA) occurs naturally, for example in human skin, as a natural metabolite of the amino acid, histidine. UCA receives a lot of attention because of evidence that its UV excitation in air affects the immune system possibly through the formation of reactive oxygen species (ROS) that are implicated in damaging skin, resulting in skin cancer [1–7]. Concurrent to its biological significance, interest grew on the nature of the excited state(s) and photochemical mechanisms involving UCA [8–11]; such as the wavelength dependence of the initial *trans* to *cis* isomerization [4]. Reports on the formation of singlet oxygen from electronically excited UCA are of particular interest because of the high reactivity of singlet oxygen with sensitive biological systems. Evidence for singlet oxygen formation included product studies [1,12], and observation of luminescence at 1270 nm [5,13]. Theoretical methods have also been applied to the photosensitization mechanisms and photoisomerization of UCA [14–16]. While the sensitized production of singlet oxygen and subsequent TYPE II reactions appear to be a possible or even usual reaction pathway on substrates from UV-excited UCA, these reactions may not prevail in all cases. The cholesterol hydroperoxide assay test for singlet oxygen formed on photoexcitation of UCA in air yielded the 7α-ChOOH isomer as well as 5α-ChOOH, the former indicative of a free radical, TYPE I process [9]. Also the inhibition by Trolox of the photo-peroxidation of methyl linoleate (ML) in sodium dodecyl sulfate (SDS) micelles is indicative of a TYPE I process [17]. The possible reactions become complicated due to direct oxidation reactions of UCA itself. Direct oxidation of UCA by the riboflavin triplet rather than singlet oxygen accounted for the inactivation of glucose 6-phosphate dehydrogenase [18] and UCA isomers were reported to be "good" hydroxyl radical scavengers [19,20] and to trap peroxyl radicals, although much more slowly than does Trolox [21].

On considering some simple chemical systems to clarify the possible photo-oxidation reactions due to photo-excited UCA, we were reminded by the late C.S. Foote that the "significant competition which determines whether TYPE I or TYPE II reaction occurs is thus between substrate and oxygen for triplet sensitizer" [22]. In

* Corresponding author. Tel.: +1 506 364 2369; fax: +1 506 364 2313.
E-mail address: rbarclay@mta.ca (L.R.C. Barclay).

1010-6030/$ – see front matter © 2009 Elsevier B.V. All rights reserved.
doi:10.1016/j.jphotochem.2009.08.008

addition to this "competition", it is possible that the nature of the system employed may dramatically affect the pathway of the main reactions. For example, electronically excited benzophenone, which is well known to be an excellent H-atom abstractor, switches to give energy transfer to oxygen and TYPE II products when the donor substrate and benzophenone are "phase-separated" by a narrow air gap [23]. In biological systems, analogous separations, such as between aqueous and lipid phases, could have a profound effect on reactions initiated by photo-excited states. Consequently the main objective of this investigation was to determine the effect, if any, of different media on the mechanisms of photo-oxidation initiated by UCA and its methyl ester. Accordingly we now report on experiments employing UCA or its methyl ester, UCAME, in several different systems including homogeneous solution and systems often used to mimic the natural molecular environment such as heterogeneous aqueous-lipid media of micelles and lipid bilayers. It was first necessary to determine if UCAME exhibited hydrogen atom transfer (HAT) activity in its ground state since it contains a free N–H group and might act as a HAT donor towards peroxyl radicals similar to the behavior of some pyrroles [24]. An unsaturated lipid, the linoleate chain, was selected as a substrate for a series of photo-initiated experiments since this lipid is known to give specific kinetics of peroxidation [25–27] and known products [23,28–30] typical of a free radical (TYPE I) or of a singlet oxygen reaction (TYPE II) depending on which pathway predominates. The photo-initiated reactions were carried out in homogeneous solution, in micelles of SDS, in lipid bilayers of dimyristoylphosphatidylcholine (DMPC) containing methyl linoleate as substrate and in bilayers of dilinoleoylphosphadtidylcholine (DLPC).

The methods used to investigate the pathways of the peroxidations included kinetic studies of oxygen uptake along with the effects of antioxidants or singlet oxygen quenchers, as appropriate, and product analyses of linoleate hydroperoxides to test proposed reaction pathways.

2. Materials and methods

2.1. General

Solvents used, common chemicals and antioxidants were of highest quality from Aldrich. Antioxidants were re-crystallized from methanol before use and stored at −20 °C. Sodium dodecyl sulfate (SDS) was electrophoresis purity obtained from BIO-RAD. The phospholipids, dimyristoyl- and dilinolylphosphatidylcholine (DMPC and DLPC) were obtained form Avanti Polar Lipids in sealed vials on "dry ice" and stored below −20 °C. Methyl linoleate (ML) was obtained from NuCheck Prep in sealed vials under nitrogen. It was determined to be hydroperoxide free just before use by TLC analysis on silica gel developed with heptane/ethyl acetate (8/2, v/v). For this purpose parallel TLC analyses were run on the new ML compared to a sample partly oxidized. The hydroperoxides were detected with *N,N*-dimethyl-1,4-phenylenediamine dihydrochloride spray (in methanol/water/acetic acid, 100/25/1, v/v/v) and compared to the observed TLC position of the peroxide-free ML detected by a spray of 1.5% ceric ammonium nitrate in 10% sulfuric acid. This latter sprayed TLC detected both ML and oxidized ML. NMR spectra were determined on a JOEL 270 MHz Spectrometer, mass spectra on a HP 5988A instrument using a GLC interface and 12m capillary column and UV/vis spectra on a Varian Cary Bio 100 Spectrometer. HPLC analyses were carried out on a Varian 9050/9012 system with an auto-sampler. An adsorption phase column, 25 cm × 5 mm, generally 10 μm silica, was used with a flow rate of 1.5–2.0 ml/min unless other wise indicated. The oxidation products from ML were identified by reduction with triphenylphosphine followed by HPLC analysis of their corresponding hydroxyl compounds using the solvent mixture hexane/2-propanol//acetone (992/4/4, v/v/v) and confirmed by comparison of their HPLC with a known sample from an independent laboratory as described earlier [26].

Phosphate buffer was prepared from de-ionized distilled water containing 0.01 phosphate buffer saline from SIGMA passed through a column of Chelex 100 resin (BIO-RAD) that was conditioned with the buffer to pH 7.4–7.6. Diethylenetriaminopentaacetic acid, 1.4×10^{-4} M, was then added to complex traces of heavy metal ions. This buffer will be referred to as PBS.

2.2. Trans-urocanic (UCA) and methyl urocanate (UCAME)

Trans-UCA (Aldrich), re-crystallized from methanol/water (30/10, v/v) gave m.p. 225 °C (rapid dec., lit. m.p. 223–225 °C dec. [3]). Conversion to UCAME was carried out by acid catalysis in methanol by the published procedure [12]. The crude product was re-crystallized from ethyl acetate and further purified by sublimation *in vacuo* to yield a colorless solid, m.p. 100–101 °C (lit. m.p. 100–101 °C [31]. The mass spectrum showed the parent ion at M^+ 152 (*rel. inten.* 45) and major fragment ions at *m/e* 121 (*rel. inten.* 100) and 93 (*rel. inten.* 71). The ^{1}H NMR spectrum was consistent with that reported [12].

2.3. Autoxidation and photo-initiated procedures

The oxygen uptake studies were carried out at 30 or 37 °C at 760 Torr in air using a sensitive, calibrated, dual-channel apparatus that is described elsewhere [32]. Photo-initiated reactions were initiated through Pyrex using a 200 W super pressure mercury lamp, the relative intensity of which was monitored throughout each run by fiber optics sampling of the light beam with a phototube detector. A series of neutral density filters of known transmittance mounted on a filter wheel were used to change light intensities.

2.4. Preparations of aqueous/lipid dispersions

Solutions of ML, PMHC and DBHA of known concentrations in 0.50 M SDS/PBS were prepared by vortex stirring under nitrogen to give clear solutions just before use. Trolox was prepared and used in PBS. Multilamellar vesicules (MLV) of DMPC or DLPC containing known amounts of additives as required (ML, UCAME) were prepared by co-evaporation to films followed by vortex stirring and 10 freeze–thaw cycles in liquid nitrogen as reported earlier [27]. Unilamellar vesicles (ULV) were prepared in Tham buffer (pH 7.0) by extrusion of MLV through micron filters under nitrogen (five times with 0.40 μm, twice through two 0.10 μm and finally four times through 0.05 μm filters). The ^{31}P NMR spectra of the vesicles were determined on a JEOL 270 MHz instrument at 109.25 MHz by the pulse sequence reported earlier [33]. The MLV vesicles exhibited the typical very broad anisotropic ^{31}P NMR signal (50 ppm) while the ULV showed a simple narrow signal [33]. Supporting Material includes traces of the ^{31}P spectra of the MLV and ULV vesicles and ^{1}H NMR spectra of UCA and UCAME.

3. Results

3.1. Quantitative kinetic studies and product analysis to distinguish free radical (TYPE I) and singlet oxygen (TYPE II) pathways of photo-oxidations

The kinetics and mechanism of free radical autoxidation have been discussed in several reviews (e.g. [34,35]). In general, these most common reactions of organic substrates usually involve either initiation by peroxyl radicals in thermal reactions or excited triplet states in photo-initiated reactions and take place in a sequence of

initiation, propagation, and termination steps. For *uninhibited reactions*, the general kinetic expression of oxygen uptake which applies to these reactions is given by Eq. (1),

$$\frac{-\mathrm{d}[O_2]}{\mathrm{d}t} = \frac{k_p}{(2k_t)^{1/2}} \times [R_sH] \times R_i^{1/2} \quad (1)$$

where k_p and $2k_t$ are the rate constants for radical chain propagation and termination respectively, R_sH the substrate, and R_i is the rate of free radical initiation. These reactions are generally inhibited by antioxidants (typically substituted phenols) which terminate the reaction of peroxyl radicals by reactions (2) and (3).

$$ROO^\bullet + ArOH \xrightarrow{k_p} ROOH + ArO^\bullet \quad (2)$$

$$ROO^\bullet + ArO^\bullet \rightarrow \text{nonradicalproducts} \quad (3)$$

Antioxidants suppress the oxygen uptake for a length of time, τ, which is related to the R_i by Eq. (4), where n, the stoichiometric factor, is the number of radicals trapped per molecule of antioxidant, generally 2.0 for phenolic antioxidants [34].

$$R_i = \frac{n[ArOH]}{\tau} \quad (4)$$

If the stoichiometric factor is unknown, it can be determined by measuring the R_i with a known antioxidant in a separate experiment and the n determined for the unknown by the use of Eq. (4). During *inhibited oxidations*, the oxygen uptake is given by Eq. (5).

$$\frac{-\mathrm{d}[O_2]}{\mathrm{d}t_{inh}} = \frac{k_p}{k_{inh}} \times [R_sH] \times \frac{R_i}{n}[ArOH] \quad (5)$$

Integrating Eq. (5) provides Eq. (6) for the incremental oxygen uptake.

$$-\Delta[O_2]_t = \frac{k_p}{k_{inh}} \times [R_sH] \ln\left(1 - \frac{t}{\tau}\right) \quad (6)$$

For reactions which obey these equations, a plot of $-\Delta[O_2]_t$ versus $\ln(1 - t/\tau)$ will give a linear slope of $k_p[R_sH]/k_{inh}$ from which the absolute rate constant for inhibition, k_{inh}, is obtained provided the propagation rate constant, k_p, for the substrate is known or can be determined. Alternately, where there is sufficient oxygen uptake at the beginning of the induction period, the initial $-\mathrm{d}[O_2]/\mathrm{d}t_{inh}$ can be estimated and the k_{inh} calculated using the differential equation (5).

In photo-initiated oxidations the rate of oxygen consumption is determined by the light intensity and, assuming there is no "dark reaction", this kinetic order of the rate should be proportional to the half power of the light intensity since this controls the R_i in Eq. (1). This relationship has been found to apply in several systems, including those relevant to the current investigation in micelles [26,29] and lipid bilayers [27]. In addition, reactions propagated by oxygen-centered radicals are expected to be inhibited by phenolic antioxidants. Consequently the reaction kinetic order in light intensity and the effect of antioxidants are both used to test the role of the TYPE I mechanism (see Section 3.3).

Reactions initiated by singlet oxygen are *not* expected to exhibit a one-half reaction kinetic order in light intensity. As postulated earlier [23], the rate of such photo-oxidation reactions are expected to be directly related to the steady state concentration of singlet oxygen and therefore show a first order relationship for oxygen uptake with light intensity. This simple kinetic relationship has been found to hold for several systems and combined with the effects of a singlet oxygen quencher, such as sodium azide, provided evidence for the role of singlet oxygen in photo-initiated lipid peroxidation [17,30].

Analysis of oxidation products from the natural lipid linoleate is a well-known method to distinguish the roles of TYPE I versus TYPE II reaction pathways [23,28–30] bearing in mind that secondary photo-reactions on initially formed hydroperoxides [36] or quenching of the photo-reactor by additives may complicate the results [37]. The general Scheme 1 outlines the different reaction pathways for TYPE I and TYPE II oxidations on the linoleate chain. A more complete mechanism of TYPE I reactions is given in [38]. TYPE I reactions on linoleate are initiated by hydrogen atom transfer (HAT) from the reactive methylene at position 11 followed by rapid reaction with oxygen at the carbon-centered radical forming peroxyl radicals and by chain-propagating HAT on the substrate and subsequent rearrangements of peroxyl radicals leading to mixtures of *cis,trans* and *trans,trans* 9- and 13-hydroperoxides in which the ratios (*c,t* to *t,t*; *kinetic to thermodynamic* product ratios) depend on the H-atom donating ability of the medium(e.g. substrate concentration or added antioxidants). In contrast, TYPE II singlet oxygen reactions produce hydroperoxides directly in kinetically controlled reactions. Reaction by $^1O_2$ at the more reactive *bis*-allylic position 11 produces an excess of *cis,trans* conjugated hydroperoxide isomers [39] (Scheme 1, **1** and **2**) and, since the more reactive singlet oxygen is not selective, attack also occurs at the allylic Hs at positions 8 and 14 leading to non-conjugated hydroperoxides (**5** and **6**). So overall, singlet oxygen leads to a more complex reaction mixture of at least six hydroperoxides. In the absence of a powerful antioxidant, a negligible amount of the non-conjugated isomer, **7**, forms [38]. In both kinds of reactions, the products can be separated and quantified by HPLC, usually after reduction to their corresponding hydroxyl derivatives. Some examples of product analyses are given in Section 3.3.

3.2. Urocanic acid, UCA, or its methyl ester, UCAME, as antioxidants

As indicated in Section 1, it was necessary to re-examine the possibility that UCA or UCAME exhibits antioxidant activity as implied in several reports [19–21]. Since these compounds are used in this investigation as potential hydrogen atom acceptors or energy transfer agents in their excited states, any powerful hydrogen atom transfer (HAT) reactions from their ground states might mask or complicate the study. To check for possible HAT activity in UCAME we selected the classical thermal initiation by the azo-initiator, AIBN, in the hydrocarbon cumene as substrate because in this system of very low k_p [40] even very weak (HAT) antioxidants (e.g. 2,6-di-*tert*-butyl-4-methoxy phenol DBHA) [34] give well-defined inhibition periods [41]. An example of such an experiment, shown in Fig. 1, indicates very clearly that UCAME does not possess any detectable inhibition of the oxygen uptake whereas the weak antioxidant, DBHA, stopped the oxygen uptake almost completely. However the literature examples employed UCA, not an ester, and this may explain some of the differences observed (see Section 4).

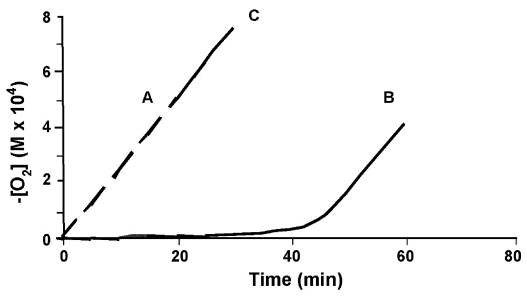

Fig. 1. Oxygen uptake profile for the oxidation of cumene, 5.36 M, in chlorobenzene initiated by AIBN, 0.0198 M, at 30 °C. (A) Uninhibited reaction; (B) inhibited by 2,6-di-*tert*-butyl-4-methoxyphenol (DBHA), 2.25×10^{-6} M; (C) effect of methyl urocanate (UCAME), 2.69×10^{-5} M.

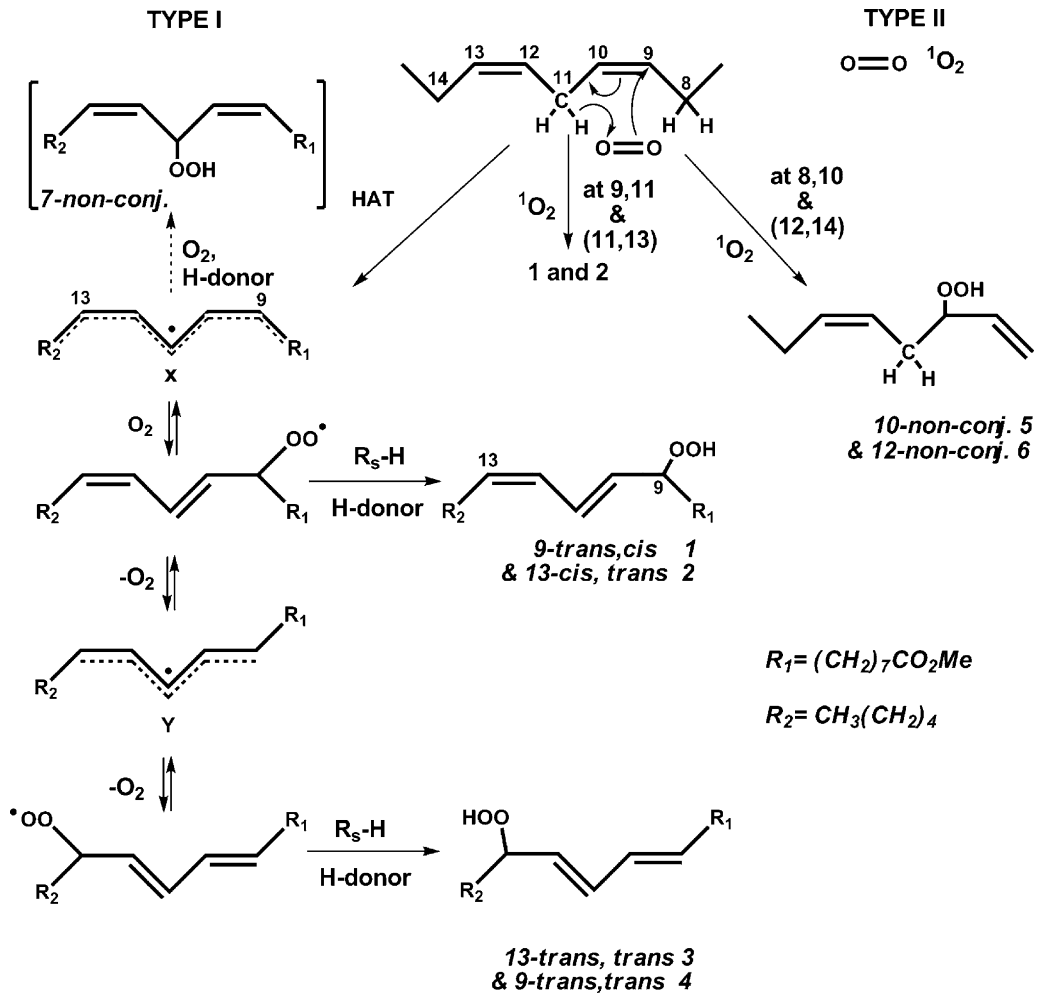

Scheme 1.

3.3. Photo-initiated peroxidation of methyl linoleate in solution

3.3.1. Evidence for TYPE I reactions

Kinetic studies of photo-irradiation using methyl linoleate (ML) as substrate in non-protic solvents provided clear evidence that UCAME readily initiates TYPE I photo-oxidation. A typical example of these results is shown in Fig. 2A and B. Toluene was selected as the solvent for solubility purposes and it was necessary to show that this solvent was inert to UV irradiation in the presence of UCAME and air as indicated in Fig. 2A. Then on the addition of ML there is rapid oxygen uptake which was efficiently inhibited by antioxidants, even by the comparatively weak inhibitor, DBHA, as shown in Fig. 2B. Not surprisingly, singlet oxygen quenchers such as β-carotene did not reduce the oxidation, Fig. 2A, trace B (dotted line) and a relatively high concentration of the quencher, 1,4-diazabicyclo[2.2.2]octane, DABCO, 2.0×10^{-4} M, similarly showed no effect on the oxygen uptake.

The oxygen uptake rates were followed for seven different light intensities. The resulting linear plot shown in Fig. 3 results in a kinetic order in oxygen uptake versus light intensity of approximately one-half. This reaction kinetic order is expected of free radical oxidation and together with the above results establishes a classical, TYPE I, free radical peroxidation pathway.

Product studies were carried out to complete the results for UCAME-sensitized peroxidation of ML in toluene solution. The hydroperoxides were reduced with triphenyl phosphine immediately after the reaction and the products analyzed as their

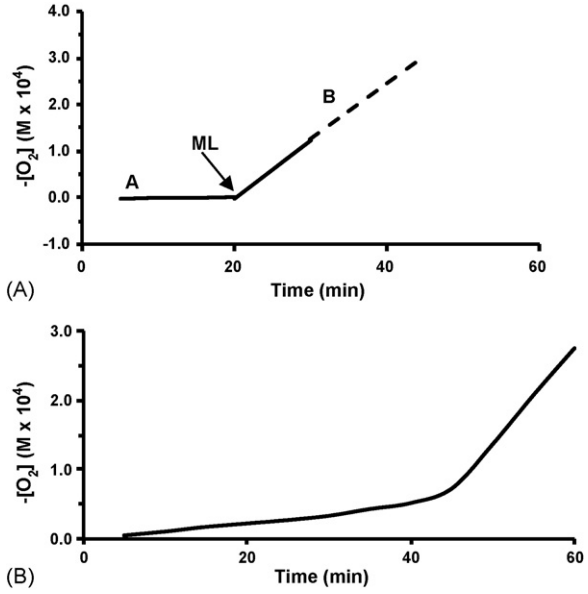

Fig. 2. (A) Oxygen uptake profile for the peroxidation of methyl linoleate (ML), 0.45 M, in toluene at 30 °C, photo-initiated initiated by UCAME, 2.30 mM. (A) UV light on without ML, ML added at 20 min.; (B) effect of β-carotene 4.07×10^{-5} M. DABCO, 2.0×10^{-4} M, has no effect on the oxygen uptake (not shown). (B) Inhibited by DBHA, 8.94×10^{-6} M.

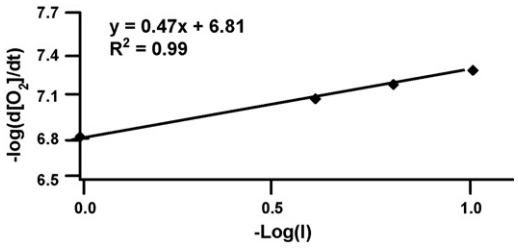

Fig. 3. Kinetic order plot for the effect of UV light intensity on the peroxidation of ML, 0.45 M, photo-initiated by UCAME, 2.30 mM in toluene at 30 °C. The kinetic order = 0.47 with R^2 = 0.99.

corresponding hydroxyl derivatives. A comparable experiment was carried out employing benzophenone as the photo-initiator, a well-known H-atom abstractor via its triplet state [26], and comparative chromatograms using benzophenone and UCAME are shown in Fig. 4A and B. The results showing the four main products, the two *cis,trans* and two *trans,trans* hydroxy-substituted isomers are typical of the TYPE I radical peroxidation of linoleate. The slightly higher *c,t* to *t,t* isomer ratio found with ucame-sensitized photo-initiation (0.39) compared to that with benzophenone (0.30) is expected because the higher ML concentration (0.695 M versus 0.483 M) is expected to increase this kinetic to thermodynamic product ratio [26,42].

Since our objective was to evaluate the role of free radical peroxidation versus singlet oxygen reactions on linoleate, it was desirable to carry out some kinetic experiments and product studies involving singlet oxygen for comparison purposes. For this purpose we used dye-sensitized oxidation in solution, a well-known method to generate singlet oxygen [23,28]. A kinetic order experiment of oxygen uptake versus light intensity for methylene blue-sensitized oxidation of methyl linoleate in solution is shown in Supporting Material (SM), Fig. S3, where the kinetic order of approximately unity is typical of a singlet oxygen reaction [23].

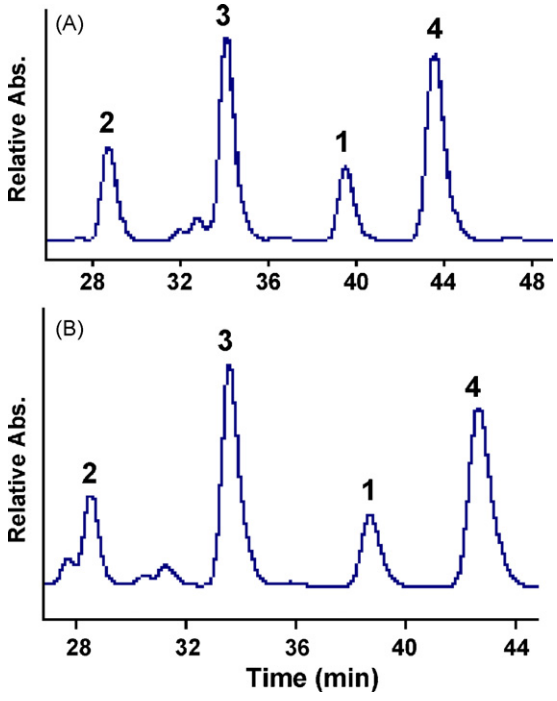

Fig. 4. HPLC analyses of the oxidation products of ML, as the hydroxyl derivatives; **2**, 13-hydroxy-*cis,trans*, **3**, 13-hydroxy-*trans,trans*, **1**, 9-hydroxy-*trans,cis* and **4**, 9-hydroxy-*trans,trans* isomers in order of elution. (A) Reaction initiated by UV irradiation of benzophenone 4.99 mM in heptane on ML 0.483 M. *Cis,trans*//*trans,trans* isomeric ratio = 0.30 ± 0.03 at 37 °C. (4) Reaction initiated by UV irradiation of UCAME, 10.8 mM in toluene on ML 0.695 M. *Cis,trans*//*trans,trans* isomeric ratio = 0.39 ± 0.05.

Earlier product studies from methylene blue-sensitized oxidation of ML gave a product profile where the two *cis,trans* isomers **1** and **2** (Scheme 1) dominated the products formed resulting in a *c,t* to *t,t* ratio of 14 [23]. A similar experiment was repeated herein by photo-initiated oxidation of ML with methylene blue in chlorobenzene (not shown) which gave a comparable result with a *c,t* to *t,t* isomer product ratio of 16.

3.4. Photo-initiated peroxidation of ML in sodium dodecyl sulfate (SDS) micelles by UCAME and by UCA: antioxidant activities in micelles

Aqueous micelles such as SDS have provided a useful model for experiments on thermal or photo-initiated peroxidations in heterogeneous aqueous/lipid systems [26,43,44]. Such systems can be used to initiate oxidation from the aqueous phase or from the lipid phase. The ester, UCAME, was sparingly soluble in organic solvents but dissolved readily in 0.50 M SDS, suggesting that it partitions into the micellar/lipid phase as does ML [26]. Therefore a photo-oxidation of the combination SDS/ML/UCAME was carried out using different light intensities and the result of such an experiment is shown in SM, Fig. S4. The observed kinetic order of one-half for oxygen uptake versus light intensity is similar to that found earlier with photo-initiation of linoleic acid peroxidation by benzophenone in a TYPE I reaction [26,42]. These results from kinetic studies with UCAME are thus very similar to those found from benzophenone photo-initiated peroxidation of linoleic acid in SDS micelles [26]. For comparison purposes, it was of interest to examine the effect of light intensity on the oxidation of ML on the combination SDS/ML/UCA prepared by adding a buffer solution of UCA to a ML/SDS solution. The resulting kinetic order, approximately one-half, is shown in SM, Fig. S5 and indicates that both excited UCAME and UCA initiate TYPE I reactions.

Since the results from photo-initiation using UCA as well as UCAME in SDS micelles support the TYPE I mechanism, we investigated more fully the use of the water-soluble UCA as photo-initiator to compare the antioxidant capacities of typical phenolic antioxidants. The use of this form of the compound provided more flexibility in designing experiments since it can be added from aqueous buffer in varying amounts to provide measurable oxygen uptake during the UV radiation. By this method we obtained results to compare the inhibiting effects of three common phenolic antioxidants on the inhibition of lipid peroxidation: PMHC, a powerful antioxidant of the hydroxyl chromanol (vitamin E) class [45], DBHA, a hindered phenol and commercial antioxidant, both added from known concentrations prepared in SDS micelles, and Trolox, a water-soluble compound of the vitamin E class. Trolox has the advantage of water-solubility and consequently has been frequently used in clinical trials and to compare the efficacy of other antioxidants, so that it is not surprising to find that SciFinder Scholar currently gives at least 1000 references to "Trolox as antioxidant". The structures of these antioxidants are shown in Fig. 5.

A typical experiment illustrating oxygen uptake during photolysis of the SDS/ML/UCA combination and inhibition by PMHC is illustrated in Fig. 6 showing the uninhibited rate, curve A, the inhibiting effect of PMHC, curve B, and an inset, C, a plot of $-\Delta[O_2]$ versus $\ln(1 - t/\tau)$. This linear plot shows that the inhibition profile follows the classical kinetics of Eq. (6). The antioxidants DBHA and Trolox also exhibited antioxidant activity during photo-initiation by UCA in aqueous SDS and the effects of the three antioxidants on the inhibited oxygen uptake are compared qualitatively in Fig. 7.

There is significant oxygen uptake during the induction periods for all three antioxidants compared to typical results in non-protic solvents (see Figs. 1 and 2) which qualitatively indicates low

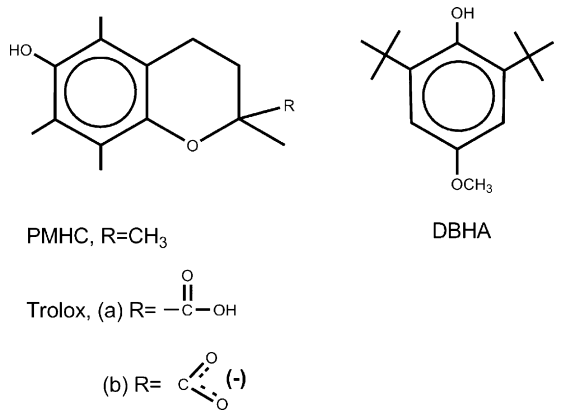

Fig. 5. Structures of the antioxidants used: PMHC, Trolox, and DBHA.

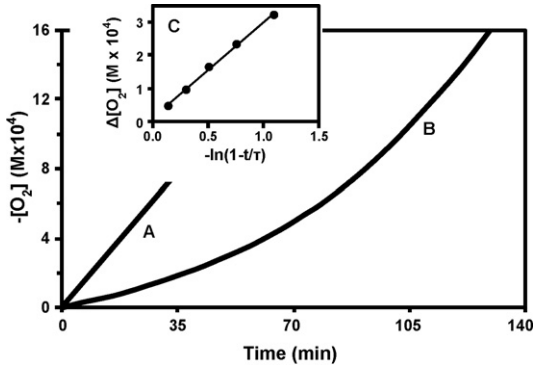

Fig. 6. Oxygen uptake profiles for the peroxidation of ML, 0.60 M, in SDS, phosphate buffer, pH 7.4, photo-initiated by UCA, 0.492×10^{-4} mol at 30 °C. (A) Uninhibited reaction; (B) inhibited with PMHC, 61 μM (calcd. for SDS phase); (C) inset of the data from B plotted according to the linear equation (6).

antioxidant activities in the aqueous SDS medium. By repetition of these experiments with the three antioxidants, their antioxidant activities were determined by measurement of their absolute rate constants for inhibition, k_{inh}, and these are summarized in Table 1. Their stoichiometric factors, n, were calculated relative to $n = 2$ for PMHC [34] by determination of the R_i by measurement of the induction period using PMHC under the same conditions and n calculated using Eq. (4). Additional details of these experiments are given in SM, Table S1. The relative antioxidant activities are, Trolox ≥ PMHC > DBHA. The stoichiometric factors, n, for PMHC

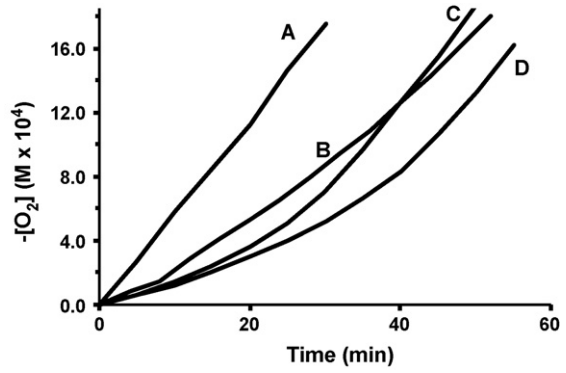

Fig. 7. A qualitative comparison of the effect of antioxidants on the peroxidation of ML, 0.60 M, photo-initiated by UCA, 0.492×10^{-4} mol in SDS, phosphate buffer, pH 7.4 at 30 °C. (A) Uninhibited reaction; (B) inhibited with DBHA, 21 μM; (C) inhibited with PMHC, 20 μM; (D) inhibited with Trolox, 21 μM (assuming that Trolox is completely partitioned into the SDS micellar phase).

Table 1
Antioxidant activities, k_{inh}, and stoichiometric factors, n, of phenolic antioxidants during inhibited peroxidation of methyl linoleate (ML)[a] photoinitated by urocanic acid (UCA)[b] in 0.50 M sodium dodecyl sulfate (SDS) at 30 °C in saline phosphate buffer, pH 7.4.

Antioxidant[c]	k_{inh} ($M^{-1}\,s^{-1} \times 10^{-3}$)[d]	n[e]
PMHC	50.4 ± 5.0	2.0
DBHA	31.7 ± 0.9	1.9[e]
Trolox	60.3 ± 7.8	1.7 ± 0.1

[a] The concentration of ML was 0.60 M in the SDS phase where the micellar volume was calculated to be 2.50×10^{-4} l per 2.00 ml of 0.50 M SDS [26].
[b] Experiments generally used 50 μM UCA, except one run with Trolox used 25 μM.
[c] Concentrations of antioxidants in the micellar phase ranged for PMHC, 25.2–136.4 μM, DBHA, 20.6–61.7 μM, Trolox, 20.9–54.5 μM.
[d] The rate constants from at least three experiments were calculated using Eq. (5) from the initial rate of oxygen uptake, $-d[O_2]/dt_{inh} = k_p/k_{inh} \times [ML]R_i/n[ArOH]$, using $k_p = 36\,M^{-1}\,s^{-1}$ [26] and the R_i measured for each experiment using PMHC; $R_i = 2 \times [PMHC]/\tau$. The R_i and induction period, τ, for each experiment are given in Supporting Material (SM). Error limits were determined at 95% confidence interval for k_{inh}.
[e] From two measurements.

and DBHA both are approximately 2, whereas the value for Trolox, which is introduced from the aqueous phase, is about 15% less. It distributes only partially into 0.10 M SDS ($f = 0.19$ [26]) and presumably partially into 0.50 M SDS as used herein, therefore some of the Trolox is probably wasted due to competing radical reactions in the aqueous phase (see Section 4). Overall the antioxidant activities of these typical phenols are dramatically different in aqueous micellar media compared to known values in a non-protic solvent [45]. Briefly, their k_{inh} values are both leveled and marked reduced in aqueous SDS. For example, in styrene the value for PMHC in styrene is 75 times and that for DBHA 3.5 times of that shown here in aqueous/SDS. The values in aqueous micelles are not only greatly reduced but are similar (Table 1) between these three antioxidants in contrast to the values in styrene [45]. Several effects including solvation by water and the unique effects of a micellar environment itself appear to be operating to cause these reductions in observed antioxidant activities in aqueous micelles (see Section 4).

3.5. Peroxidation of lipid bilayers photo-initiated by UCA from the aqueous phase

Micelles are known to be dynamic species which undergo rapid breaking and reforming which allows for rapid exchange of monomers [46]. In contrast, lipid bilayers form more stable aggregates in water and phosphatidylcholine bilayers are often selected as models of natural membranes since they mimic much of the structural type and physical properties of natural membranes. Consequently it was anticipated that such a boundary between the aqueous and lipid phases might provide a system that would exhibit competition between TYPE I and TYPE II reactions.

3.5.1. Photo-initiated peroxidation of ML in dimyristoylphosphatidylcholine (DMPC) bilayers by UCA

The system selected for these experiments, was methyl linoleate (ML), the oxidizable substrate, contained in multilamellar vesicles (MLV) consisting of saturated lipid chains from DMPC. This is an appropriate system to compare/contrast with the kinetic results obtained with the combination of ML in SDS micelles. Also the concentration of the oxidizable lipid, ML, can be controlled in this mixture and some kinetic evidence is available on this system from earlier thermal-initiated peroxidation studies [25].

The results from photo-initiation of the combination ML/DMPC in bilayers by UCA contrasted with those for the combination of photo-initiation by UCA in ML/SDS micelles or in homogeneous solution by UCAME. The contrasts are shown in Fig. 8 for the bilayer

system compared, for example, to Fig. 6 or 7 in micelles. In micelles, antioxidants were effective inhibitors but the water-soluble singlet oxygen quencher, sodium azide, exhibited no effect on oxygen uptake, whereas in ML/DMPC initiation with UCA was *not* affected by Trolox, the better antioxidant in the SDS system, but sodium azide proved to be effective at reducing oxidation. This effect was also found to be dependent on the concentration of sodium azide added as shown in the experiment summarized in Fig. 8, Inset. The profile of reduced oxidation was non-linear in this system showing a greater reduction during the first additions of quencher.

The ML/DMPC dispersions used were quite turbid so that filtered light at the lower intensities did not provide reproducible rate measurements, however kinetic results were obtained for four different intensities. A plot of such data shown in SM, Fig. S6 indicates a first order in rate of oxidation with light intensity. Consequently the kinetic evidence overall supports a TYPE II mechanism. It is quite clear that a change in the type of heterogeneous aqueous/lipid dispersion from micellar to bilayer AND initiation with water-soluble UCA has resulted in a change of mechanism from TYPE I to TYPE II.

Since UCA is reported to undergo photoinduced decomposition in oxygen as well as isomerization [1,11,15] and UCAME readily adds generated singlet oxygen [12], it is somewhat surprising that the kinetic studies give constant uptakes of oxygen for our kinetic order and/or inhibition experiments where the irradiation times were often prolonged to several hours. Therefore a study was made of the UCA concentrations at the beginning and during several of these experiments by scanning the UV/vis through the range 200–400 nm. All samples were diluted by methanol by the identical amount to keep absorbance in the range 0.200–0.500 where they showed the general absorption typical of UCA with λ_{max} 277–278 nm. The reference side of the spectrometer contained a reference sample without UCA prepared from the same concentration of ML/SDS (or ML with DMPC) diluted with methanol to the same extent. The initial analysis were made by removing samples starting before radiation (T-0) and at various stages during the run. However it was soon found that there was no change in the UCA absorbance during the run. The remaining samples were taken from the final solution after the run and compared to the T-0 sample. In the experiments using the ML/SDS system, 93–97% of the UCA remained after the photo-initiation, while a typical sample from the ML/DMPC bilayer system, 99% of the UCA remained after the run. A control experiment carried out on UV/vis irradiation of UCA in SDS but without ML showed that 93% of UCA remained after 30 min irradiation and after 4 h this dropped to 84% of the UCA at T-0. The persistence of UCA through a run was fortuitous since it

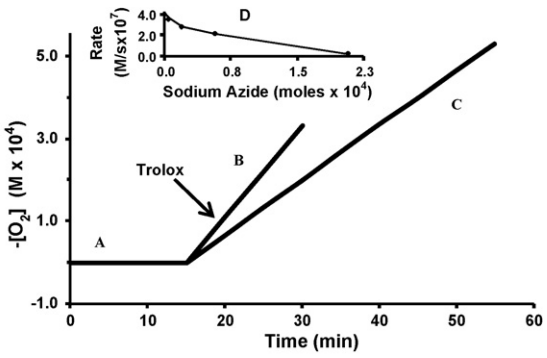

Fig. 8. Oxygen uptake profiles for the peroxidation of ML, 1.20×10^{-4} mol, in initiated by UCA, 5.80×10^{-5} mol, in phosphate buffer, pH 7.4 at 37 °C. (A) UV light on dimyristoylphosphatidylcholine (DMPC) multilamellar bilayers, 2.60×10^{-4} mol, photo with DMPC and UCA without ML; (B) in the presence of ML; the arrow shows the addition of Trolox, 6.54×10^{-9} mol; (C) the effect of sodium azide 4.55×10^{-6} mol. The inset shows the effect of sodium azide concentration on the oxygen uptake.

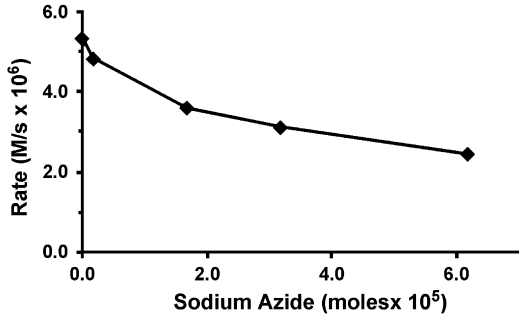

Fig. 9. Plot of the effect of sodium azide concentration on the photo-oxidation of dilinoleoylphosphatidylcholine (DLPC) multilamellar bilayers, 7.45×10^{-5} mol, initiated by UCA, 12.5×10^{-5} mol, in phosphate buffer, pH 7.4, at 37 °C.

permitted the completion of the various kinetic experiments without loss of the rate of oxygen uptake due to loss of the initiator. This is similar to previous results found on using benzophenone or azaaromatics as photo-initiators [26,29] where the initiators were regenerated during the reaction (see Section 4).

3.5.2. Photo-peroxidation of dilinoleoylphosphatidylcholine (DLPC) by UCA

Evidence given in the previous section indicated that photo-excited UCA in the aqueous phase resulted in reaction by singlet oxygen on ML encapsulated into DMPC liposomes as shown by the effect of sodium azide quencher and the kinetic order in light intensity (Fig. 8 and SM, S6). It was desirable to repeat experiments on the model membrane prepared from DLPC where the lipid chains are bonded in the bilayer structure. The DLPC bilayer is readily oxidized and used quite frequently as a model for an unsaturated membrane [34]. In one respect, the result using DLPC bilayers was very similar to that with the DMPC/ML/UCA combination. That is the oxygen uptake was reduced in much the same way with sodium azide (Fig. 9) and the oxidation was not inhibited by Trolox. However the kinetic order in light intensity was not actually first order, but 0.83 as shown in SM, Fig. S7. This unusual kinetic order may be due to other reactions that complicate the kinetics of multilamellar DLPC (see Section 4).

3.6. Photo-initiated peroxidation of dilinoleoylphosphatidylcholine (DLPC) by UCAME within the bilayer phase

Section 3.5 shows that in lipid bilayers, in contrast to micelles, photo-initiation with water-soluble UCA resulted in lipid oxidation by singlet oxygen; that is, by the TYPE II mechanism. This important result could be a consequence of the initiation and the reaction being carried out in the separate aqueous and lipid phases of the aqueous bilayers. To test this idea, we carried out an experiment to compare this result with one where the peroxidatiom of the linoleate chain is carried out with the initiator and substrate in the *same* phase. This was done by incorporating the lipid-soluble ester, UCAME, within the lipid phase of DLPC by co-evaporating the two from methanol, a common procedure used in such cases [27]. The results from a typical experiment of this type is shown in Fig. 10. In this case, Trolox exhibits antioxidant activity as shown earlier for photo-initiation within the DLPC bilayer by benzophenone [27]. The oxygen uptake during the Trolox induction period is appreciable and a plot of $-\Delta[O_2]$ versus $\ln(1 - t/\tau)$ (see inset) of this inhibition according to the linear equation (6) appears to be somewhat curved compared, for example, to such a plot from the combination SDS/ML/UCA (Fig. 6, inset C). The k_{inh} of 18.8×10^3 M^{-1} s^{-1} for Trolox, calculated from the initial inhibited oxygen uptake using Eq. (5) and the k_p of 36.1 for DLPC [27], is

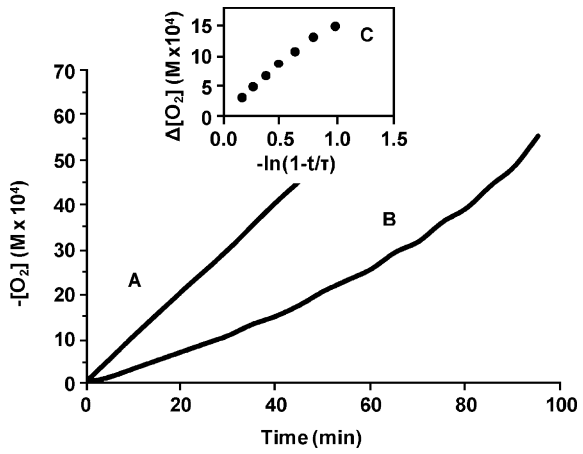

Fig. 10. Oxygen uptake profiles for the photo-oxidation of DLPC bilayers, 5.11×10^{-5} mol, photo-initiated at 37 °C by UCAME, 3.42×10^{-5} mol, by co-evaporation form methanol; (A) uninhibited reaction; (B) inhibited by Trolox, 6.32×10^{-9} mol; (C) inset of a the data from B plotted according to the linear equation (6).

markedly lower than found in solution or even in micelles (Table 1) and demonstrates the effect that this heterogeneous aqueous/lipid system has on the inhibition reaction (see Section 4).

The oxidation rates in MLV-DLPC initiated by UCAME were relatively slow in part due to the high turbidity of the MLV system. However smaller unilamellar vesicles (ULV) are known to give greater rates of oxidation [27]. The ^{31}P NMR spectrum of the MLV-DLPC showed a very broad signal, chemical shift anisotropy of 40 p.p.m., typical of such MLV particles ([56] and references therein). After several extrusions of this DLPC containing UCAME by co-evaporation the ^{31}P spectrum changed to a single line typical of smaller ULV-DLPC (see SM, Fig. S8A and B).This ULV-DMPC gave much more rapid oxidation which proved useful in efficient isolation of sufficient amounts of linoleate hydroperoxides for analyses as corresponding hydroxyl derivatives. *Trans* methylation and reduction by TPP of the isolated products [27] gave sufficient mixed hydroxy methyl linoleates for HPLC analyses and the four isomers formed were those typical of a TYPE I peroxidation (see SM, Fig. S9). These mixed isomers showed a high *c,t*/*t,t* isomer ratio, approximately 1.54 (average of two determinations, 1.51, 1.57), compared to our results in solution and even in SDS micelles. This ratio is well known to depend on the concentration of the linoleate and the temperature of the oxidation [42]. In addition the isomer ratio appears to depend on the type of bilayer particle (see Section 4). However the products formed during peroxidation are entirely consistent with the kinetic data; both results indicate a classical TYPE I reaction photo-initiated with UCAME inside the lipid phase.

4. Discussion

4.1. Thermal and photochemical results: UCA and UCAME in homogeneous solution

On the question of antioxidant activity of UCA (or UCAME), the observation that UCA reacts readily with hydroxyl radicals [19,20] does not signify that it is a radical chain-breaking antioxidant. As emphasized earlier, the vast majority of organic compounds react very rapidly with this very reactive radical [47]. The first real test of UCA as a trap of the main chain-carrying radicals in autoxidation, namely peroxyl radicals, detected some low antioxidant activity of UCA, only 400 times less efficient than Trolox [48]. We could not detect HAT activity from UCAME in cumene solution even compared to the weak antioxidant, DBHA (Fig. 1). It is quite possible that the small antioxidant effect observed for UCA in a polar, aqueous medium [48] could be due to single electron transfer (SET) or proton-coupled electron transfer (PCET) [24]. However we did not detect any antioxidant activity by UCA in aqueous-phosphate buffer solutions used in our experiments.

The ester, UCAME, dissolves in non-protic solvents and was considered to be an appropriate compound for evaluating the possible HAT activity in its excited state. All experiments showed clearly that photo-excited UCAME initiated a TYPE I free radical peroxidation reaction on methyl linoleate (ML) under these conditions. This process is shown by the inhibiting effect of an antioxidant (Fig. 2A and B) and the one-half kinetic order in oxygen uptake (Fig. 3) in contrast with the kinetic order of unity for a reaction initiated by singlet oxygen (SM, Fig. S3). In addition the TYPE I pathway with UCAME was confirmed by the typical product analysis profile (Fig. 4B) where the *cis,trans* to *trans,trans* (*c,t*//*t,t*) isomer ratio contrasted with known results from reaction with singlet oxygen where the analysis is dominated by the *cis,trans* isomers **1** and **2** [23].

4.2. Photo-peroxidation of ML by UCAME and by UCA in aqueous-SDS micelles: factors controlling antioxidant activities in aqueous micelles

The ester, UCAME, dissolved readily in 0.50 M SDS by vortex stirring and presumably is incorporated into the micellar phase along with ML [26]. Irradiation of these solutions with different light intensities gave a kinetic order of oxygen uptake with light intensity of one-half (SM, Fig. S4) indicative of the HAT-TYPE I mechanism in the micellar phase. The comparable result in kinetic order of oxygen uptake from photo-oxidation of the combination SDS/ML/UCA by simply injecting UCA into the aqueous phase (SM, Fig. S5) indicates a TYPE I pathway for both methods and this was supported by inhibition studies (*vide infra*).

Photo-peroxidation of ML in SDS was readily initiated by injection of UCA into the aqueous phase and these reactions were inhibited by three typical antioxidants (Figs. 6 and 7). The photochemical method has certain advantages over the more conventional method employing thermal initiators; namely: (i) corrections to the measured oxygen uptake required for thermal azo-initiators due to nitrogen evolution are not needed, (ii) convenient control of the oxygen uptake rates and the rate of radical initiation chain, R_i, are possible by changing the light intensity and (iii) any thermal reaction can be checked with the light off. Consequently reliable results were obtained for the absolute rate constants of antioxidant activities, k_{inh}, and stoichiometric factors, n, for the typical antioxidants PMHC, Trolox and DBHA as summarized in Table 1.

Aqueous micelles have been used frequently as heterogeneous aqueous-lipid phases to mimic natural biochemical systems for measurements of antioxidant activities [26,43,44]. The measured antioxidant activities are well known to be markedly reduced and leveled in aqueous media compared to those in non-polar solvents and this *solvent effect* has been extensively investigated ([49], and references therein). In a homogeneous protic solvent, the solvent effect can be attributed to hydrogen bonding by solvent at the phenolic hydroxyl group preventing attack by peroxyl radicals in the rate-determining step (Scheme 2) [49].

It has been recognized for some time that the reduction of phenolic antioxidant activities in aqueous-lipid heterogeneous lipid

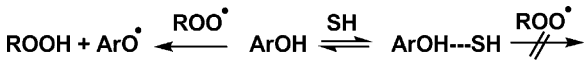

Scheme 2.

systems cannot be explained entirely by hydrogen bonding [50,51]. The reductions in antioxidant activities could be due to the nature of the particular lipid system itself which would cause rate-limiting diffusion [50] or result in physical inaccessibility between the peroxyl radical and the antioxidant [51]. However the effect of H-bonding can be evaluated separately since quantitative studies by Ingold and co-workers has provided a relationship which permits actual calculations of rate constants for H-atom abstraction by radicals in protic solvents [52]. Their Eq. (7), permits calculation of the HAT rate constant, k_s, in any H-bonding accepting (HBA) solvent from the rate constant in a non-H-bonding solvent, k^0, and known thermodynamic parameters [53]; namely, the H-bonding donating ability of the donor antioxidant, α_2^H, and the H-bond accepting ability of the solvent, β_2^H.

$$\log(k^s/\mathrm{M^{-1}\,s^{-1}}) = \log(k^0/\mathrm{M^{-1}\,s^{-1}}) - 8.3\alpha_2^H\beta_2^H \quad (7)$$

It is of interest to apply this equation to the current kinetic data and evaluate the relative effects of H-bonding by the water and specific micellar effects on the HAT activities of the antioxidants. For this purpose some relevant data is given in Table 2.

This shows: (i) required literature rate constants for PMHC, Trolox and DBHA in a non-H-bonding solvent, k^0 in styrene; (ii) the calculated and experimental results, k^{calc}_{MeOH} and k^{exp}_{MeOH}, in methanol, a common H-bonding solvent, to test the method used here and (iii) $k^{calc}_{H_2O,SDS}$ and $k^{exp}_{H_2O,SDS}$ for our current results on PMHC and Trolox. The method is not applicable to highly hindered phenols like DBHA since the α and β parameters are not determined. To calculate k^{calc}_{MeOH} for PMHC in methanol we used the α_2^H available for α-tocopherol, 0.370 [52], since the chromanol structures are the same and their antioxidant activities are very similar, within 16%, in homogeneous solution [45]. For calculations in aqueous micelles, we used the β value, of 0.31, determined for water since water is expected to be the main HBA to the phenolic hydroxyl in aqueous micelles [51]. The calculated k^{calc}_{MeOH} is in reasonable agreement with the experimental value. However the measured value in aqueous SDS, $5.0 \times 10^4\,\mathrm{M^{-1}\,s^{-1}}$, is markedly different by more than eight times lower than the calculated value, $42 \times 10^4\,\mathrm{M^{-1}\,s^{-1}}$. This means that only a very small part of the reduction in antioxidant activity can be attributed to hydrogen bonding by water in this system, much of the effect must be due to the effect of the micellar system which can reduce the rate either by restricted diffusion between the lipid peroxyl radicals and antioxidant and/or compartmentalization of the lipid peroxyl radical relative to the antioxidant. The α value for Trolox is not known, however it is very probable that the large reduction in k_{inh} for Trolox in aqueous micelles is also due mainly to the micellar environment rather than hydrogen bonding. Compared to other vitamin E class of phenolic antioxidants Trolox exhibits much lower antioxidant activity in non-polar solvents (3.5 times lower than PMHC, Table 2) yet it at least matches this activity in SDS micelles at pH 7.4. This switch is attributed to the presence of an electron-attracting carboxyl group in the non-polar solvent (Fig. 5, Trolox A) which destabilizes the intermediate phenoxyl radical of the rate-determining step (reaction (2)). In contrast this group will be a carboxylic anion (Fig. 5, Trolox B) at pH 7.4 which is electron supplying to stabilize the intermediate. The Swain field effect parameter provides a measure of these opposite effects, for COOH, $F = 0.552$ and for COO^-, $F = -0.221$) [54], where a negative value indicates an electron-supplying effect while a positive value an electron-attracting effect.

Table 2
Rate constants, k_{inh} ($\times 10^{-4}\,\mathrm{M^{-1}\,s^{-1}}$) for PMHC, Trolox and DBHA in a non-polar solvent, k^0, compared to calculated and experimental (k^{calc} and k^{exp}) values in methanol and, in water/SDS.

	Antioxidant		
	PMHC	Trolox	DBHA
$k^0_{styrene}$ [a]	380	110	11
k^{calc}_{MeOH}	47 [b]		
k^{exp}_{MeOH}	57 [b]		
$k^{calc}_{H_2O,SDS}$	42		
$k^{exp}_{H_2O,SDS}$	5.0	6.0	

[a] Rate constants are taken from Ref. [45].
[b] From Ref. [24].

4.3. Photo-peroxidation of linoleate in lipid bilayers by UCA and UCAME: TYPE II versus TYPE I reactions

As indicated in Section 3, the system consisting of ML sequestered in bilayers of DMPC containing saturated lipid chains was used for photo-initiated experiments to compare with the classical results for earlier thermal free radical peroxidation [25] and in particular with results herein for photo-peroxidation of ML by UCA in SDS micelles. The results from photo-peroxidation from the combination DMPC/ML/UCA stand in sharp contrast with both the free radical peroxidation in solution and the photo-initiated reactions in the system SDS/ML/UCA in micelles. The reactions clearly proceeded in the DMPC bilayers by attack with singlet oxygen since they were not inhibited by the antioxidant, Trolox, which is generally very effective to inhibit peroxyl radical attack in this system [25], and the oxidation was effectively reduced by sodium azide (Fig. 8). In addition a TYPE II process is supported by a kinetic order of unity in oxygen uptake with light intensity (SM, Fig. S6).

It is somewhat fortuitous that UCA is not consumed by the active oxygen species (AOS) in these reactions in micelles or bilayers. In this regard the results resemble the earlier result when benzophenone was used as photo-initiator [26,29]. So from analogy we propose that there is a pathway to regenerate the UCA during the reaction. This is illustrated in Scheme 3. In this scheme the reactions are initiated from the ^{3}n,π*state of UCA [11] from which reaction can take two pathways: (i) energy transfer may form singlet oxygen which diffuses into bilayers to cause singlet oxygen products directly whereas (ii), in solution or micelles the prominent reaction is hydrogen transfer from a active C–H bond of linoleate starting a TYPE I free radical process and generating a reactive UCA-H•. The latter is expected to react readily with either lipid peroxyls to form observed LOOH products or oxygen (or both) to release HOO• radicals into the aqueous phase. These could react with Trolox and also account for the lower stoichiometric factor observed for Trolox compared to that for PMHC (Table 1).

A very important question remains. Why do the different media, like aqueous/lipid bilayers and aqueous/lipid micelles result in such markedly different reaction pathways? To explain these different results, we consider the essential differences between homogeneous solutions and micelles on the one hand compared to lipid bilayers on the other. In solution it is obvious that the UCA (UCAME) excited state will collide freely with ML the give a HAT reaction. In micelles, which are also continuously providing rapid exchange at least of small molecules like UCA (but some restricted diffusion of hydrophobic molecules, e.g. ML), there is also sufficient molecular contact between excited UCA and ML to generate mainly a HAT process but with lower efficiency compared to homogeneous solution. The difference in bilayers is attributed to the very significant difference with lipid bilayers where there is a boundary/barrier between the aqueous and lipid phases. This is shown schematically in Scheme 4. When UCA is excited in the aqueous phase, molecular contact between excited UCA and ML/bilayer is prevented but the small reactive oxygen species, singlet oxygen, like oxygen, can diffuse sufficiently into the bilayer to cause a TYPE II reaction. This

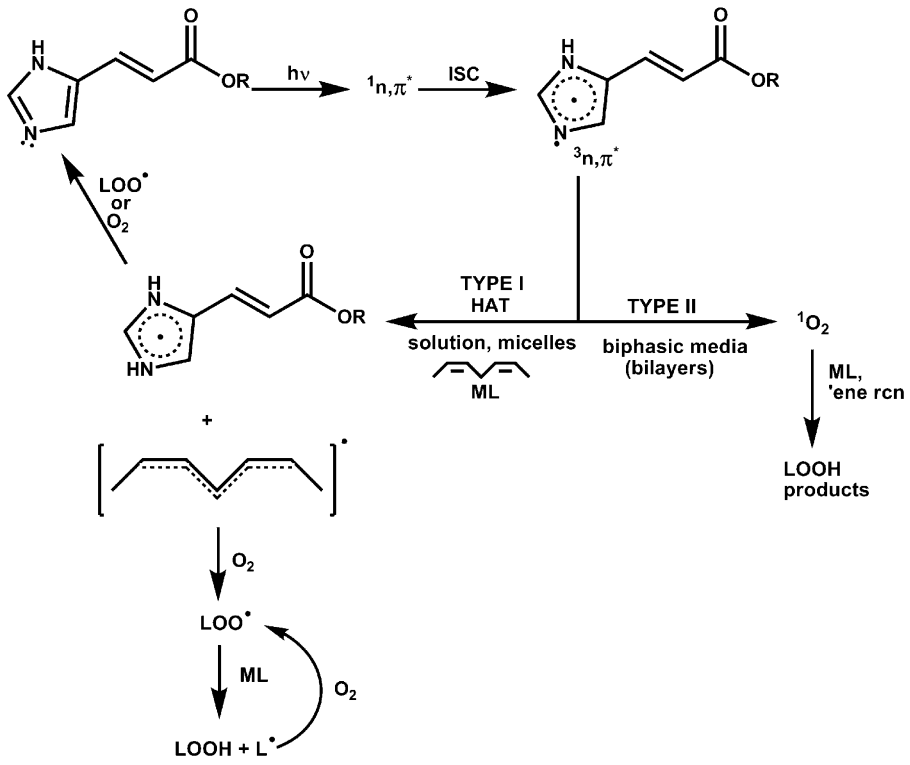

Scheme 3.

is analogous to the earlier observation where light-irradiation of bilayers containing methylene blue in the aqueous phase produced singlet oxygen products by diffusion of singlet oxygen into the lipid phase [30].

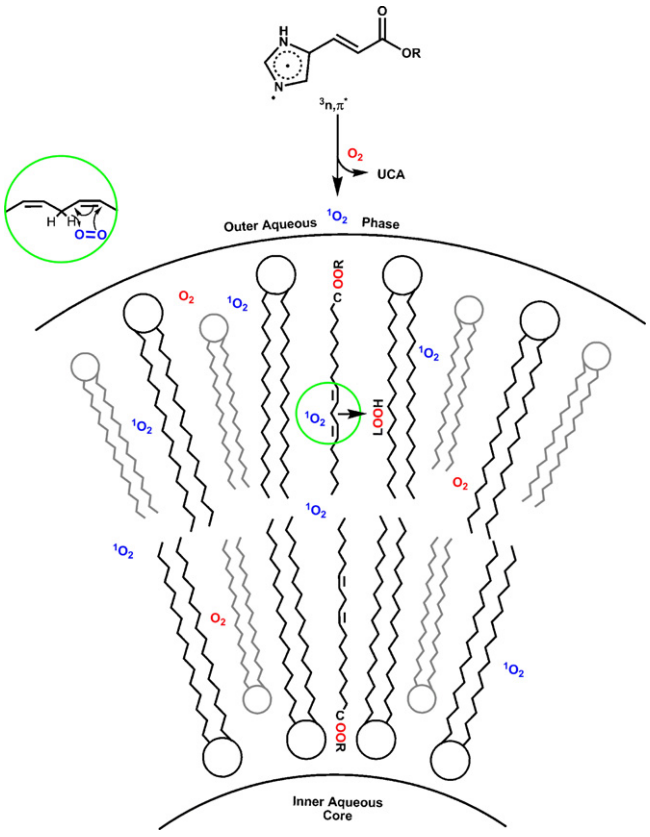

Scheme 4.

The simple model of Scheme 4 should also account for the recent observation that UCA can distribute partially into bilayers, at least into egg lecithin [55]. It is proposed that UCA, which is in the form of the charged anion, is probably *not* incorporated deep into the hydrophobic region of the bilayers but is likely bound near the polar surface.

Assuming that the ML lipid is situated as shown in Scheme 4 with the polar ester group near the polar surface, the photo-excited UCA will not reach the unsaturated region of ML to initiate HAT at the reactive methylene site. To test this hypothesis, it was helpful to carry out the opposite experiment where the photo-initiator is located within the hydrophobic region of the bilayer. Photo-oxidation of this system was inhibited by Trolox (Fig. 10) indicative of a HAT-type reaction.

Some product analysis results were in agreement with this oxygen uptake-inhibition result. The significant result from product analysis from the ULV-DLPC/UCAME photo-oxidation is formation of the four *c,t*//*t,t* isomer combination typical of the TYPE I (HAT) reaction. The high *c,t*//*t,t* ratio, 1.54, found is somewhat higher than expected since at 37 °C this ratio from DLPC was in the range of 1.2–1.3 for radical peroxidations initiated by either a lipid-soluble [42] or water-soluble thermal initiator [56]. The complete characterization of the extruded DLPC is beyond the scope of this investigation. However the higher *c,t*//*t,t* but it is probably due to the smaller particle size of the extruded DLPC (presumably at least partly ULV according to the ^{31}P NMR spectrum). Several studies have concluded that the "packing" of the lipid chains is tighter in the inner mono-layer [57–59]. In addition the "arm-to-arm" propagation observed for DLPC [60] is expected to be significant in closely packed chains. The result of these two factors would be to favor H-atom abstraction by the initially formed peroxyl radical leading to the *t,c* (*c,t*) isomers (Scheme 2, **1** and **2**) in competition with β-scission leading to the *t,t-isomers* **3** and **4** [42]. So the two contrasting results, photo-oxidation of the bilayer combinations (1) DMPC/ML/UCA (or DLPC/UCA) and conversely (2) DLPC/UCAME illustrate the very important effect that different media such as lipid

bilayers, compared to homogeneous solution or micelles, have in controlling the photo-oxidation reaction pathways in such aqueous/lipid systems.

Various observed non-ideal results of kinetic behavior of MLV bilayers such as the kinetic order observed for the system DLPC/UCA (SM, Fig. S7) and the non-linear plot according to Eq. (6) for the system DLPC/UCAME/Trolox (Fig. 10) can be attributed to the heterogeneity within the bilayer. In the latter example, the k_{inh} ($18.8 \times 10^4\ M^{-1}\ s^{-1}$) extracted from the early part of the induction period is not reliable probably due to photo-oxidation occurring deep within the MLV system before Trolox has distributed uniformly throughout the system. Reactions other than propagation by peroxyl radicals and their self-termination could complicate the results. For example, the recent report of hydroxyl radical generation during azo-initiated peroxidation of methyl linoleate leading to a lipid ketone could affect both kinetic and product studies, especially if this reaction "is more probable in membranes" as suggested [61].

5. Conclusions

The formation of singlet oxygen by UV irradiation of urocanic acid (UCA) is very well documented and the potential damaging effect on human skin has been a major concern. However the detection of singlet oxygen from electronically excited UCA by energy transfer to oxygen does not necessarily mean that the electronically excited oxygen results in TYPE II singlet oxygen reactions under all conditions. In general competition can exist between a target molecule and oxygen for the excited state with a resulting competition between TYPE I, free radical processes, and TYPE II by singlet oxygen. It is clear from the results herein that urocanic acid in its $^3n,\pi^*$ excited state is capable of exhibiting hydrogen atom abstraction from organic substrates containing weak C–H bonds such as unsaturated lipids in systems where *direct contact* between UCA and the substrate is possible such as in homogeneous solution or in dynamic aqueous/lipid mixtures like micelles. In the presence of oxygen in these fluid systems, free radical reactions of the TYPE I process are initiated. In contrast, when the UCA is isolated from direct contact with the organic substrate; for example, when UCA is irradiated in the aqueous phase of lipid bilayers, energy transfer to oxygen forms singlet oxygen and this competing reaction can dominate leading to typical TYPE II reactions rather than free radical reactions.

Kinetic methods and product studies of lipid hydroperoxides provide useful methods to distinguish between these two main reaction pathways initiated photochemically in solution and in aqueous/lipid mixtures. Antioxidants are commonly applied to studies in polar solvents and in heterogeneous lipid/aqueous systems wherein hydrogen bonding by solvents greatly reduce their antioxidant activity. Such effects can be predicted by quantitative methods of "solvent effects". However in hydrophobic regions of micelles and of lipid bilayers other factors, such as diffusion limiting behavior, may dominate antioxidant activities and the reduction of antioxidant activities are much greater than can be predicted. In order to determine the intrinsic antioxidant activity of antioxidants, it is advisable to first determine their activities in a non-polar solvent where these effects are absent.

The potential dual effects of UV-excited UCA are of particular significance for the protection of human skin against damaging UV radiation. The simple model systems used in this study may have significant implications when considering the processes in more complex natural biological media. In real biological systems, a knowledge of the singlet oxygen and of the free radical reactions should both be considered in a strategy for protection against UV radiation [62].

Supporting material

Supporting Material available includes: (1) Table S1, with additional details of the kinetic data for the peroxidation of methyl linoleteate in SDS micelles inhibited by phenolic antioxidants; (2) ^{1}H NMR spectra of urocanic acid and methyl urocanate, Figs. S1 and S2; (3) kinetic order plots of oxygen uptake with UV light intensity during photo-oxidation of methyl linoleate under different conditions, Figs. S3–S5; (4) kinetic order plots of oxygen uptake with UV light intensity during peroxidation of methyl linoleate in DMPC bilayers photo-initiated by urocanic acid, Fig. S6, and of DLPC bilayers photo-initiated by methyl urocanate, Fig. S7; (5) ^{31}P NMR spectra of multilamellar and of unilamellar, DLPC bilayers Fig. S8; (6) HPLC trace of the product isomers from photoperoxidation of DPLC by methyl urocanate, Fig. S9.

Acknowledgements

We thank the staff of our Department who provided technical help in this investigation, Danny Durant, Philip Cormier, Roger Smith, and Patt Wilson. L.R.C.B. acknowledges receipt of a Discovery Grant in support of this research from the Natural Sciences and Engineering Council of Canada (NSERC) and A.A.R. acknowledges receipt of an Undergraduate Student Award from NSERC.

Appendix A. Supplementary data

Supplementary data associated with this article can be found, in the online version, at doi:10.1016/j.jphotochem.2009.08.008.

References

[1] E.L. Menon, H. Wasserman, Formation of singlet oxygen by urocanic acid by UVA irradiation and some consequences thereof, Photochem. Photobiol. 75 (2002) 565–569.
[2] A. Kammeyer, S. Pavel, S.S. Asghar, J.D. Bos, M.B.M. Teunissen, Prolonged increase of *cis*-urocanic acid in human skin and urine after single total-body ultraviolet exposures, Photochem. Photobiol. 65 (1997) 593–598.
[3] T. Mohammad, H. Wasserman, H. HogenEsch, Urocanic acid photochemistry and photobiology, Photochem. Photobiol. 69 (1999) 115–135.
[4] K.M. Hanson, B. Li, J.D. Simon, A spectroscopic study of the epidermal ultraviolet chromophore *trans*-urocanic acid, J. Am. Chem. Soc. 119 (1997) 2715–2721.
[5] K.M. Hanson, J.D. Simon, Epidermal *trans*-urocanic acid and the UV-A-induced photoaging of the skin, Proc. Natl. Acad. Sci. U.S.A. 95 (1998) 10576–10578.
[6] J.D. Simon, Spectroscopic and dynamic studies of the epidermal chromophores *trans*-urocanic acid and eumelanin, Acc. Chem. Res. 33 (2000) 307–313.
[7] K.M. Hanson, R.M. Clegg, Observation and quantification of ultraviolet-induced reactive oxygen species in *ex vivo* human skin, Photochem. Photobiol. 76 (2002) 57–63.
[8] B. Li, K.M. Hanson, J.D. Simon, Primary processes of the electronic excited states of *trans*-urocanic acid, J. Phys. Chem. 101 (1997) 969–972.
[9] N. Haralampus-Grynaviski, C. Ransom, T. Ye, M. Rôżanowska, M. Wrona, T. Sarna, J.D. Simon, Photogeneration and quenching of reactive oxygen species by urocanic acid, J. Am. Chem. 124 (2002) 3461–3468.
[10] W.L. Ryan, D.H. Levy, Electronic spectroscopy and photoisomerization of *trans*-urocanic acid in a supersonic jet, J. Am. Chem. 123 (2001) 961–966.
[11] T. Mohammad, Laser-induced invitro isomerization of urocanic acid in UV A region and the origin of excited triplet state, Tetrahedron Lett. 43 (2002) 8897–8900.
[12] R. Roa, K.E. O'Shea, Reactions of urocanic acid (UCA) methyl esters with singlet oxygen and 4-methyl-1,2,4-triazoline-3,5-dione (MTAD), Tetrahedron 62 (2006) 10700–10708.
[13] J. Baier, T. Maisch, M. Maier, E. Engel, M. Landthaler, W. Bäumler, Singlet oxygen generation by UVA light exposure of endogenous photosensitizers, Biophys. J. 91 (2006) 1452–1459.
[14] L. Shen, H.-F. Ji, Theoretical investigation of the photosensitization mechanisms of urocanic acid, J. Photochem. Photobiol. B: Biol. 91 (2008) 96–98.
[15] O. Dmitrenko, W. Reischl, R.D. Bach, J. Spanget–Larsen, TD-DFT Computational insight into the origin of wavelength-dependent E/Z photoisomerization of urocanic acid, J. Phys. Chem. 108 (2004) 5662–5669.
[16] J. Danielsson, J. Uličný, A. Laaksonen, A TD-DFT study of the photochemistry of urocanic acid in biologically relevant ionic, rotameric, and photometric forms, J. Am. Chem. Soc. 123 (2001) 9817–9821.
[17] L.R.C. Barclay, M.C. Basque, V.C. Stephenson, M.R. Vinqvist, Photoxidations initiated or sensitized by biological molecules: singlet oxygen versus radical

peroxidation in micelles and human blood plasma, Photochem. Photobiol. 78 (2003) 248–255.
[18] E. Silva, L. Herrera, A.M. Edwards, J. de la Fuenta, E. Lissi, Enhancement of riboflavin-mediated photo-oxidation of glucose 6-phosphate dehydrogenase by urocanic acid, Photochem. Photobiol. 81 (2005) 206–211.
[19] A. Kammeyer, T.A. Eggelte, J.D. Bos, M.B.M. Teunissen, Urocanic acid isomers are good hydroxyl radical scavengers: a comparative study with structural analogues and with uric acid, Biochim. Biophys. Acta 1428 (1999) 117–120.
[20] A. Kammeyer, T.A. Eggelte, H. Overmars, A. Bootsma, J.D. Bos, M.B.M. Teunissen, Oxidative breakdown of urocanic acid isomers by hydroxyl radical generating systems, Biochim. Biophys. Acta 1526 (2001) 277–285.
[21] C. López-Alarcón, A. Aspée, C. Henríquez, A.M. Campos, E.A. Lissi, Interaction and reactivity of urocanic acid towards peroxyl radicals, Redox Report 10 (2005) 227–234.
[22] C.S. Foote, Photosensitized oxidation and singlet oxygen: consequences in biological systems, in: W.A. Pryor (Ed.), Free Radicals in Biology, vol. II, Academic Press, New York, 1976, pp. 85–133.
[23] L.R.C. Barclay, M.-C. Basque, M.R. Vinqvist, Singlet-oxygen reactions sensitized on solid surfaces of lignin or titanium dioxide: product studies from hindered secondary amines and from lipid peroxidation, Can. J. Chem. 81 (2003) 457–467.
[24] P.D. Maclean, E.R. Chapman, S.L. Dobrowolski, A. Thompson, L.R.C. Barclay, Pyrroles as antioxidants: solvent effects and the nature of the attacking radical on antioxidant activities and mechanisms of pyrroles, dipyrrinones, and bile pigments, J. Org. Chem. 73 (2008) 6623–6635.
[25] L.R.C. Barclay, S.L. Locke, J.M. MacNeil, J. VanKessel, Quantitative studies of the autoxidation of linoleate monomers sequestered in phosphatidylcholine bilayers. Absolute rate constants in bilayers, Can. J. Chem. 63 (1985) 2633–2638.
[26] L.R.C. Barclay, K.A. Baskin, S.J. Locke, T.D. Schaefer, Benzophenone-photosensitized autoxidation of linoleate in solution and sodium dodecyl sulfate micelles, Can. J. Chem. 65 (1887) 2529–2540.
[27] L.R.C. Barclay, K.A. Baskin, K.A. Dakin, S.J. Locke, M.R. Vinqvist, The antioxidant activities of phenolic antioxidants in free radical peroxidation of phospholipid membranes, Can. J. Chem. 68 (1990) 2258–2269.
[28] M.J. Thomas, W.A. Pryor, Singlet oxygen oxidation of methyl linoleate: isolation and characterization of the NaBH4-reduced products, Lipids 15 (1980) 544–548.
[29] L.R.C. Barclay, E. Crowe, C.D. Edwards, Photo-initiated peroxidation of lipids in micelles by azaaromatics, Lipids 32 (1997) 237–245.
[30] L.R.C. Barclay, J.K. Grandy, H.D. MacKinnon, H.C. Nicol, M.R. Vinqvist, Peroxidations initiated by lignin model compounds: investigating the role of singlet oxygen in photo-yellowing, Can. J. Chem. 76 (1998) 1805–1816.
[31] T. Mohammad, H. Morrison, A convenient synthesis of *cis*-urocanic acid, an endogenous immunosuppressant, OPPI Briefs 32 (2000) 581–584.
[32] D.D.M. Wayner, G.W. Burton, Handbook of Free Radicals and Antioxidants in Biomedicine, CRC Press, Boca Raton, FL, 1989, pp. 223–232.
[33] L.R.C. Barclay, A.M.H. Bailey, D. Kong, The antioxidant activity of α-tocopherol-bovine serum albumin complex in micellar and liposome autoxidations, J. Biol. Chem. 260 (1985) 15809–15814.
[34] L.R.C. Barclay, M.R. Vinquist, Phenols as antioxidants, in: Z. Rappoport (Ed.), The Chemistry of Phenols, John Wiley and Sons, Ltd., Chichester, England, 2003, pp. 839–908.
[35] G.W. Burton, K.U. Ingold, Vitamin E: applications of the principles of physical organic chemistry to the exploration of its structure and function, Acc. Chem. Res. 19 (1986) 194–201.
[36] C. Tanielian, R. Mechin, R. Seghrouchi, C. Schweitzer, Mechanistic and kinetic aspects of photosensitzation in the presence of oxygen, Photochem. Photobiol. 71 (2000) 12–19.
[37] F. Boscá, M.A. Miranda, I.M. Morea, A. Samadi, Involvement of type I and type II mechanisms in the linoleic acid peroxidation photosensitized by tiaprofenic acid, J. Photochem. Photobiol. B: Biol. 58 (2000) 1–5.
[38] B. Roschek, K.A. Tallman, C.L. Rector, J.G. Gillmore, D.A. Pratt, C. Punta, N.A. Porter, Peroxyl radical clocks, J. Org. Chem. 71 (2006) 3527–3532.
[39] C. Tanielian, R. Mechin, Reaction and quenching of singlet molecular oxygen with esters of polyunsaturated fatty acids, Photochem. Photobiol. 59 (1994) 263–268.
[40] J.A. Howard, K.U. Ingold, Absolute rate constants for hydrocarbon oxidation XII. Rate constants for secondary peroxy radicals, Can. J. Chem. 46 (1968) 2661–2666.
[41] D.V. Gardner, J.A. Howard, K.U. Ingold, The inhibition of autoxidation by 2,4,6-tri-*tert*-butyl substituted phenol, aniline, and thiophenol, Can. J. Chem. 42 (1964) 2847–2851.
[42] N.A. Porter, B.A. Weber, H. Weenen, J.A. Khan, Autoxidation of polyunsaturated lipids. Factors controlling the stereochemistry of product hydroperoxides, J. Am. Chem. Soc. 102 (1980) 5597–5601.
[43] W.A. Pryor, J.A. Cornicelli, L.J. Devall, B. Tait, B.K. Trivedi, D.T. Witiak, M. Wu, A rapid screening to determine the antioxidant potencies of natural and synthetic antioxidants, J. Org. Chem. 58 (1993) 3521–3532.
[44] L.R.C. Barclay, C.D. Edwards, K. Mukai, Y. Egawa, T. Nishi, Chain-breaking naphtholic antioxidants: antioxidant activities of polyalkylbenzochromanol, polyalkylbenzochromenol, and 2,3-dihydro-5-hydroxy-2,2,4-trimethylnaphto[1,2-b]furan compared to an α-tocopherol model in sodium dodecyl sulphate micelles, J. Org. Chem. 60 (1995) 2739–2744.
[45] G.W. Burton, T. Doba, E.J. Gabe, L. Hughes, F.L. Lee, L. Prasad, K.U. Ingold, Autoxidation of biological molecules. 4. Maximizing the antioxidant activity of phenols, J. Am. Chem. Soc. 107 (1985) 7053–7065.
[46] M. Novo, S. Felekyan, C.A.M. Seidel, W. Al-Soufi, Dye-exchange dynamics in micellar solutions studied by fluorescence correlation spectroscopy, J. Phys. Chem. B 111 (2007) 3614–3624.
[47] F. Antunes, L.R.C. Barclay, K.U. Ingold, M. King, J.Q. Norris, J.C. Scaiano, F. Xi, On the antioxidant activity of melatonin, Free Radic. Biol. Med. 26 (1999) 117–128.
[48] C. López-Alarcón, A. Aspée, C. Henriquez, A.M. Campos, E.A. Lissi, Interaction and reactivity of urocanic acid towards peroxyl radicals, Redox Report 10 (2005) 227–234.
[49] G. Litwinienko, K.U. Ingold, Solvent effects on the rates and mechanisms of reaction of phenols with free radicals, Acc. Chem. Res. 40 (2007) 222–230.
[50] L. Castle, M.J. Perkins, Inhibition kinetics of chain-breaking phenolic antioxidants in SDS micelles. Evidence that intermicellar diffusion rates may be rate-limiting for hydrophobic inhibitors such as α-tocopherol, J. Am. Chem. Soc. 108 (1986) 6381–6382.
[51] L. Valgimigli, K.U. Ingold, J. Lusztyk, Antioxidant activities of vitamin E analogues in water and a Kamlet-Taft β-value for water, J. Am. Chem. Soc. 118 (1996) 3545–3549.
[52] D.W. Snelgrove, J. Lusztyk, J.T. Banks, P. Mulder, K.U. Ingold, Kinetic solvent effects on hydrogen-atom abstractions: reliable quantitative predictions via a single empirical equation, J. Am. Chem. Soc. 123 (2001) 469–477.
[53] M.H. Abraham, P.L. Grellier, D.V. Prior, P.P. Duce, Hydrogen bonding. Part 7. A scale of solute hydrogen-bond activity based on log K values for complexation in tetrachloromethane, J. Chem. Soc. Perkin Trans. II (1989) 699–711.
[54] C.G. Swain, E.C. Lupton Jr., Field and resonance components of substituent effects, J. Am. Chem. Soc. 90 (1968) 4328–4337.
[55] A.M. Campos, C. Cárcamo, E. Silva, S. García, E. Lemp, E. Alarcón, A.M. Edwards, G. Günther, E. Lissi, Distribution of urocanic acid isomers between aqueous solutions and *n*-octanol, liposomes or bovine serum albumin, J. Photochem. Photobiol. B: Biol. 90 (2008) 41–46.
[56] L.R.C. Barclay, K.A. Baskin, D. Kong, S.J. Locke, Autoxidation of model membranes. The kinetics and mechanism of autoxidation of mixed phospholipid bilayers, Can. J. Chem. 65 (1987) 2541–2550.
[57] S.J. Marrink, A.E. Mark, Molecular dynamics simulation of the formation, structure, and dynamics of small phospholipid vesicles, J. Am. Chem. Soc. 125 (2003) 15233–15242.
[58] C.G. Brouillette, J.P. Segrest, T.C. Ng, J.L. Jones, Minimal size phosphatidylcholine vesicles: effects of radius of curvature on head group packing and conformation, Biochemistry 21 (1982) 4569–4575.
[59] J.P. Douliez, A.M. Bellocq, E.J. Dufourc, Effect of size, polydispersity and multilayering on solid state ^{31}P- and ^{2}H-NMR spectra, J. Chim. Phys. 91 (1994) 874–880.
[60] F. Antunes, L.R.C. Barclay, M.R. Vinqvist, R.E. Pinto, Determination of propagating and termination rate constants by using an extension to the rotating-sector method: application to PLPC and DLPC bilayers, Int. J. Chem. Kinet. 30 (1998) 753–767.
[61] M. Frenette, J.C. Scaiano, Evidence for hydroxyl radical generation during lipid (Linoleate) peroxidation, J. Am. Chem. Soc. 130 (2008) 9634–9635.
[62] J.L. McCullough, K.M. Kelly, Prevention and treatment of skin aging, Ann. N.Y. Acad. Sci. 1067 (2006) 323–331.